Adaptive Orthogonal Basis Scheme for OTFS

Yinhua Jia[1(✉)], Sen Wang[2], Jing Jin[2], and Hang Long[1]

[1] Wireless Signal Processing and Network Lab Key Laboratory of Universal Wireless Communications, Ministry of Education Beijing University of Posts and Telecommunications, Beijing 100876, China
jiayinhua@163.com
[2] China Mobile Research Institute, Beijing, China

Abstract. Orthogonal time frequency space (OTFS) modulation can provide significant error performance than orthogonal frequency division multiplexing (OFDM) modulation in the high-speed scenario. However, the fractional Doppler effects cause Doppler diffusion. In this paper, we analyze the Doppler diffusion from both the formula and geometric levels. In order to alleviate Doppler diffusion, we propose an adaptive orthogonal basis scheme by using the Doppler shifts feedback of the receiver. Our scheme alter the matrix of the inverse symplectic finite Fourier transform (ISFFT) by the feedback. This scheme makes it possible to estimate the channel more accurately. In the simulation results, we show that the bit error rate (BER) and block error rate (BLER) performance of our proposed scheme is not affected compared with OTFS. In addition, our scheme can work even if the Doppler domain dimension is limited and the Doppler shifts feedback of the receiver is inaccurate.

Keywords: OTFS · delay-Doppler channel · fractional Doppler effect

1 Introduction

The sixth-generation (6G) era is expected to ultra-reliable wireless communication in the high-speed scenario such as high-speed railway, vehicle-to-everything (V2X) and low-earth-orbit satellites (LEOS) communications [3,14,15]. While the orthogonal frequency division multiplexing (OFDM) modulation deployed in the fifth-generation (5G) mobile systems can achieve high spectral efficiency, it is not robust to time-varying channels with Doppler shifts [1,2,4,5,16]. In order to realize robust transmission, a new two-dimensional (2D) modulation scheme as orthogonal time-frequency space (OTFS) was proposed [1].

In OTFS, the information symbols are multiplexed in the delay-Doppler domain rather than the time-frequency domain as the OFDM [5]. The delay-Doppler domain symbols are transformed into the time-frequency domain via the inverse symplectic finite Fourier transform (ISFFT). Relying on this 2D orthogonal transform, the OTFS modulation represents the time-varying multipath channel into the delay-Doppler domain, making all transmitted symbols

F. Gao et al. (Eds.): ChinaCom 2022, LNICST 500, pp. 57–68, 2023.
https://doi.org/10.1007/978-3-031-34790-0_5

experience the quasi-stationary channel [1–5]. Furthermore, the delay-Doppler domain channel presents sparse characters since the delay and the Doppler shift of the channel are limited for a wide-band system [6–9]. In addition, the channel representation demonstrates attractive properties such as separability, compactness, and stability which have the potential to be exploited for OTFS system design [3,14,15].

The sparse character of the channel provides the possibility to estimate the delay and Doppler shift [2]. However, interference cancellation is still necessary. In the OTFS system, Raviteja *et al.* simplify the OTFS input-output relation characterizing the interference [7]. In the case of an ideal waveform, there is no inter-carrier interference (ICI) and inter-symbol interference (ISI) occurs. while inter-Doppler interference (IDI) is still present due to unavoidable fractional Doppler effects.

In this paper, we analyze the unavoidable fractional Doppler effects in the case of an ideal waveform. Further, we show the Doppler diffusion caused by fractional Doppler effects and analyze the diffusion both on the formula and geometric level. Specially, we propose an adaptive orthogonal basis scheme to alleviate this diffusion. Finally, our results show that with coding and ideal channel estimation, the bit error rate (BER) and block error rate (BLER) performances of adaptive orthogonal basis are not affected compared with OTFS. Our scheme can work even when the Doppler domain dimension is limited and the Doppler shifts feedback from the receiver is inaccurate.

The rest of the paper is organized as follows. Section 2 reviews the diagram of the OTFS system. Next, we analyze the fractional Doppler effects in Sect. 3 and propose an adaptive orthogonal basis scheme in Sect. 4. Numerical results are presented in Sect. 5 to verify the performance of our proposed scheme and our conclusions are finally shown in Sect. 6.

Notations: Boldface capital letters stand for matrices and lower-case letters stand for column vectors. The transpose, conjugate, conjugate transpose, and inverse of a matrix are denoted by $(\cdot)^T$, $(\cdot)^*$, $(\cdot)^H$, $(\cdot)^{-1}$, respectively. $\|\mathbf{s}\|$ is the ℓ_2-norm of the vector $\mathbf{s}$. $\delta(\cdot)$ denotes the Dirac delta function. $[\cdot]_N$ is the modulo operator of divider N. $\mathbf{0}$, $\mathbf{I}_L$ and $\mathbf{F}_L$ represent zero matrix, identity matrix with the order L and $L-$order normalized discrete Fourier transform (DFT) matrix, respectively. The operator diag$\{\mathbf{x}\}$ creates a diagonal matrix with the elements of vector $\mathbf{x}$.

2 System Model

We consider an OTFS system with M subcarriers with the sub-carrier bandwidth of Δf and N symbols with the length of T. The total bandwidth and total duration of OTFS system are $B = M\Delta f$ and $T_f = NT$. Moreover, the OTFS system is critically sampled $T\Delta f = 1$.

In this section, we introduce the diagram of the OTFS system. Figure 1 shows the transceiver diagram of the OTFS system [6]. The modulator first maps the delay-Doppler information symbols $x[k,l]$ to the time-frequency symbols $X[n,m]$ by using the ISFFT. Next, the Heisenberg transform is applied

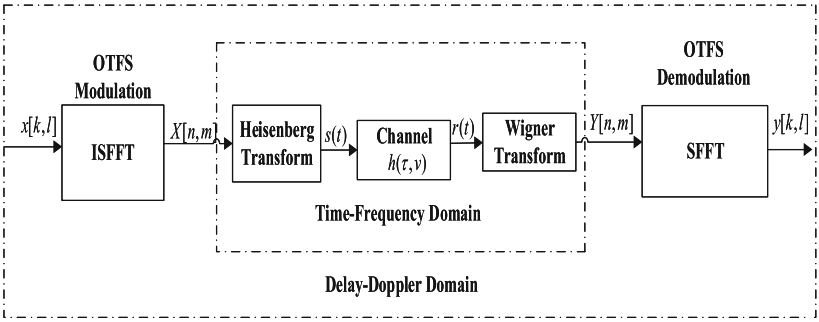

Fig. 1. The transceiver of the OTFS.

to $X[n,m]$ to generate the time domain signal $s(t)$ for transmission over the channel. At the receiver, the received time-domain signal is mapped to the time-frequency domain through the Wigner transform (the inverse of the Heisenberg Transform), and then to the delay-Doppler domain using SFFT for symbol demodulation.

In the following subsection, we will give the matrix expression of the above process from the transmitter, channel and receiver.

2.1 Transmitter

First, using the ISFFT to map the delay-Doppler information symbols to the time-frequency domain. It can be expressed as

$$\mathbf{X} = \mathbf{F}_M \mathbf{X}_{\mathbf{DD}} \mathbf{F}_N^H \tag{1}$$

where $\mathbf{X_{DD}} \in \mathbb{C}^{M \times N}$ represents the matrix form of the delay-Doppler domain symbols $x[k,l]$ and $\mathbf{X} \in \mathbb{C}^{M \times N}$ is the time-frequency domain symbol matrix.

Next, the transmitted symbols are mapped into the time domain by ultilizing the Heisenberg transform, which can be expressed as

$$\mathbf{S} = \mathbf{F}_M^H \mathbf{X} = \mathbf{X}_{\mathbf{DD}} \mathbf{F}_N^H \tag{2}$$

where $\mathbf{S} \in \mathbb{C}^{M \times N}$ is the time domain symbol matrix.

2.2 Channel

The signal $s(t)$ is transmitted over a time-varying channel with channel response $h(\tau, \upsilon)$, which characterizes the channel to an impulse with delay τ and Doppler υ [1]. The received signal is given by

$$r(t) = \iint h(\tau, \upsilon)\, s(t-\tau) \mathrm{e}^{j2\pi\upsilon(t-\tau)} \tag{3}$$

Equation (3) represents a continuous Heisenberg transform. Since typically there are only a small number of channel reflectors with associated delays and Dopplers, much more parameters are required for the delayed Doppler channel model [8,10]. The sparse representation of the channel $h(\tau, \upsilon)$ is given as

$$h(\tau, \upsilon) = \sum_{i=1}^{P} h_i \delta(\tau - \tau_i) \delta(\upsilon - \upsilon_i) \tag{4}$$

where P is the number of propagation paths, h_i, τ_i and υ_i represent the path gain, delay and Doppler shift associated with the i-th path, respectively [12,13]. The delay and Doppler for i-th path are expressed as

$$\tau_i = \frac{l_{\tau_i}}{M\Delta f}, \upsilon_i = \frac{k_{\upsilon_i} + \kappa_{\upsilon_i}}{NT} \tag{5}$$

where l_{τ_i}, k_{τ_i} are integers and real $-1/2 < \kappa_{\upsilon_i} \leq 1/2$. l_{τ_i}, k_{τ_i} represent the delay tap and Doppler tap corresponding to the delay τ_i and Doppler frequency υ_i, respectively. And κ_{υ_i} represent the fractional Doppler shift from the nearest Doppler tap k_{τ_i} [12,13].

To obtain discrete time domain representation, $s(t)$ and $r(t)$ are sampled at the interval of T/M [18], expressed by vector $\mathbf{s}$ and $\mathbf{r}$. In addition, the relation of $\mathbf{s}$ and $\mathbf{S}$ shown as

$$\mathbf{s} = vec(\mathbf{S}) \tag{6}$$

2.3 Receiver

After removal of CP at the receiver, received signal can be written as [18]

$$\mathbf{r} = \mathbf{H}\mathbf{s} + \mathbf{n} \tag{7}$$

where $\mathbf{n}$ is white Gaussion noise vector with elemental variance $\sigma_{\mathbf{n}}^2$ and $\mathbf{H}$ is the equivalent time domain channel matrix and can be represented by (4)

$$\mathbf{H} = \sum_{i=1}^{P} h_i \mathbf{\Pi}^{l_{\tau_i}} \mathbf{\Delta}^{k_{\upsilon_i} + \kappa_{\upsilon_i}} \tag{8}$$

where $\mathbf{\Pi}$ is a forward cyclic shift permutation matrix,

$$\mathbf{\Pi} = [e_2, e_3, \ldots, e_{MN}, e_1] \tag{9}$$

where e_i is the i-th column of the identity matrix $\mathbf{I}_{MN}$. $\mathbf{\Delta}$ is a diagonal matrix expressed as

$$\mathbf{\Delta} = \mathrm{diag}\{1, \mathrm{e}^{\frac{j2\pi}{MN}}, \ldots, \mathrm{e}^{\frac{j2\pi(MN-1)}{MN}}\} \tag{10}$$

We reshape $\mathbf{r}$ to received time domain symbol matrix $\mathbf{R} \in \mathbb{C}^{M \times N}$ and the matrix $\mathbf{R}$ is transformed to the delay-Doppler domain through the Wigner transform (the inverse of the Heisenberg Transform) and the SFFT respectively. It can be expressed as

$$\mathbf{r} = vec(\mathbf{R}) \tag{11}$$

$$\mathbf{Y} = \mathbf{F}_M \mathbf{R} \tag{12}$$

$$\mathbf{Y_{DD}} = \mathbf{F}_M^H \mathbf{Y} \mathbf{F}_N = \mathbf{R} \mathbf{F}_N \tag{13}$$

where $\mathbf{Y} \in \mathbb{C}^{M \times N}$ and $\mathbf{Y_{DD}} \in \mathbb{C}^{M \times N}$ are the time-frequency domain and the delay-Doppler domain received symbol matrix.

3 Fractional Doppler Effects Analysis

In Sect. 2.2, we introduce the i-th path delay and Doppler τ_i and υ_i. Since the resolution of the sampling time $1/M\Delta f$ is sufficient to approximate the path delays to the nearest sampling points in typical wide-band systems [7], we do not need to consider the fractional delay effects. However, we cannot ignore the fractional Doppler effects.

In order to analyze the fractional Doppler effects independently, we analyze the case of ideal waveforms and consider the simple channel estimation scheme [11,12]. In this scheme, we set the delay-Doppler domain symbol matrix $\mathbf{X_{DD}}_{sch}$ as

$$\mathbf{X_{DD}}_{sch}(m,n) = \begin{cases} 1, (m,n) = (0,n_k) \\ 0, others \end{cases} \tag{14}$$

$$m \in [0,1,\ldots,M-1], n, n_k \in [0,1,\ldots,N-1]$$

We recall (1) that the ISFFT process is combined by the matrix $\mathbf{F}_M$ and $\mathbf{F}_N^H$. The elements of $\mathbf{F}_N$ can be expressed as

$$\mathbf{F}_N(m,n) = \frac{1}{\sqrt{N}} \mathrm{e}^{\frac{-j2\pi mn}{M}} \quad m,n \in [0,1,\ldots,M-1] \tag{15}$$

According to (2), $\mathbf{X_{DD}}_{sch}$ is transformed to the time domain. Then transmitting through the ideal channel with $\sigma_{\mathbf{n}}^2 = 0$, (7) can be written as

$$\mathbf{r}_{sch} = \mathbf{H}\mathbf{s}_{sch} \tag{16}$$

Finally, we reshape $\mathbf{r}_{sch}$ to $\mathbf{R}_{sch}$ and obtain $\mathbf{Y_{DD}}_{sch}$ by (12) and (13),

$$\mathbf{Y_{DD}}_{sch} = \mathbf{R}_{sch} \mathbf{F}_N \tag{17}$$

where $\mathbf{Y_{DD}}_{sch}$ contains all paths channel response in the delay-Doppler domain. Focus on the i-th path channel response, it can be expressed from (10) and (15)

$$\sum_{k=0}^{N-1} \mathrm{e}^{j2\pi(\frac{(k\upsilon_i+\kappa\upsilon_i)(1+kM)}{MN})} \mathrm{e}^{j2\pi(\frac{(n_k-1-m)k}{N})} \tag{18}$$

$$= \mathrm{e}^{j2\pi\frac{k\upsilon_i+\kappa\upsilon_i}{MN}} \sum_{k=0}^{N-1} \mathrm{e}^{j2\pi\frac{(f_d'+n_k-1-m)}{N}} \tag{19}$$

where $m \in [0, N-1]$ and $k_{v_i} + \kappa_{v_i}$ represents the i-th path Doppler. Futhermore, we can derive (19) as

$$\sum_{k=0}^{N-1} \mathrm{e}^{j2\pi \frac{(k_{v_i}+\kappa_{v_i}+n_k-1-m)}{N}} = \begin{cases} N, k_{v_i} + \kappa_{v_i} + n_k - 1 - m = 0 \\ 0, k_{v_i} + \kappa_{v_i} + n_k - 1 - m \neq 0 \end{cases} \tag{20}$$

When κ_{v_i} is zero, since n_k is an integer, we have $m = k_{v_i} + \kappa_{v_i} + n_k - 1$ is also an integer. That means only one impulse in the Doppler domain according to (20). But when κ_{v_i} is not zero , m is a decimal. That means the one impulse will diffuse to the whole Doppler domain. We refer to this diffusion as the fractional Doppler effect. In practice, the diffusion is not serious when the fractional Doppler is close to 0, which is shown in the left part of Fig. 2. Conversely, the diffusion is serious when the fractional Doppler is close to 0.5, which is shown in the right part of Fig. 2.

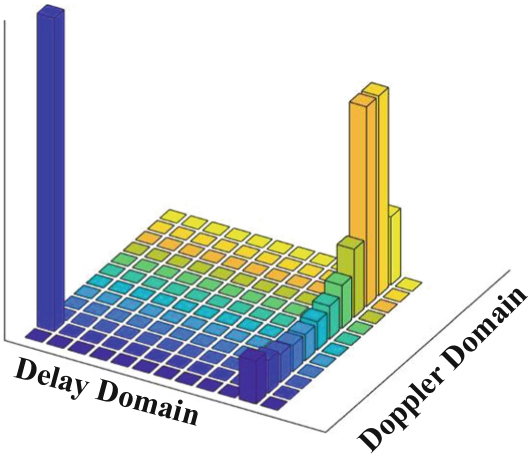

Fig. 2. Schematic diagram: $\kappa_{v_i} = 0$ and $\kappa_{v_i} = 0.5$.

Next, we try to make a geometric analysis of the Doppler diffusion. $\mathbf{F}_N$ can be regarded as a matrix composed of N orthogonal column vectors, which can be considered as channel vectors generated by N consecutive integer Doppler values. The channel estimation process can be looked upon as N vectors to represent the estimated channel vector. When the channel vector and N column vectors are not orthogonal, they cannot be represented by the matrix $\mathbf{F}_N$, so the results are serious diffusion in the Doppler domain.

4 Adaptive Orthogonal Basis Scheme

In Sect. 3, we analyze the fractional Doppler effects and serious diffusion in the Doppler domain. To alleviate this diffusion, we propose an adaptive orthogonal

basis scheme based on OTFS. In the previous section, we know the Doppler shifts of the time-varying channel are changing. If receiver feedback the Doppler shift value at a certain time and we can calculate the channel vector from it. Based on this channel vector, we use adaptive our scheme to alleviate the Doppler diffusion. In particular, even if the Doppler is changing or inaccurate, our proposed scheme can work normally within an error range.

Next, we will introduce the implementation of our scheme. Our scheme aims to alter the DFT matrix $\mathbf{F}_N$: Replace the corresponding column vector of the $\mathbf{F}_N$ with the calculated channel vector to form an orthogonal basis transformation matrix. After applying the adaptive orthogonal basis, the effect of alleviating diffusion is changed from Fig. 2 to Fig. 3.

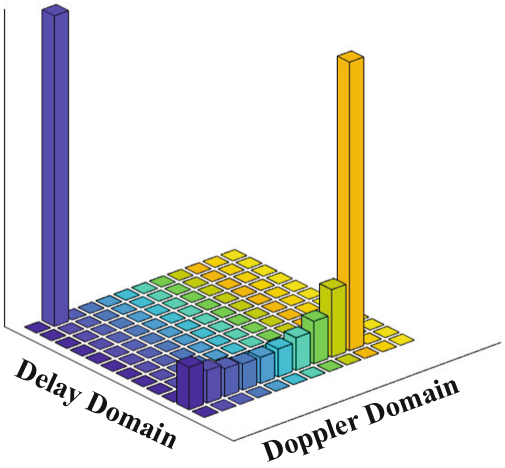

Fig. 3. Schematic diagram of adaptive orthogonal basis.

Taking the two-path channel as an example, we introduce the specific method in this scheme. We set $f_{Doppler1}$ and $f_{Doppler2}$ to represent two path Doppler shift values. According to (8) and (10), channel matrices of the two paths are expressed as

$$\mathbf{H}_1 = \begin{bmatrix} \delta^0 & \delta^M & \cdots & \delta^{(N-1)M} \\ \delta^1 & \delta^{M+1} & \cdots & \delta^{(N-1)M} \\ \vdots & \vdots & \ddots & \vdots \\ \delta^{M-2} & \delta^{2M-2} & \cdots & \delta^{NM-2} \\ \delta^{M-1} & \delta^{2M-1} & \cdots & \delta^{NM-1}, \end{bmatrix} \tag{21}$$

$$\mathbf{H}_2 = \begin{bmatrix} \xi^0 & \xi^M & \dots & \xi^{(N-1)M} \\ \xi^1 & \xi^{M+1} & \dots & \xi^{(N-1)M} \\ \vdots & \vdots & \ddots & \vdots \\ \xi^{M-2} & \xi^{2M-2} & \dots & \xi^{NM-2} \\ \xi^{M-1} & \xi^{2M-1} & \dots & \xi^{NM-1}, \end{bmatrix} \tag{22}$$

where $\delta = e^{\frac{j2\pi f_{Doppler1}}{MN}}$ and $\xi = e^{\frac{j2\pi f_{Doppler2}}{MN}}$. Then, we perform the singular value decomposition (SVD) of channel matrices. It can be expressed as

$$\mathbf{H}_1 = \mathbf{U}_1 \mathbf{\Sigma}_1 \mathbf{V}_1^T \tag{23}$$

$$\mathbf{H}_2 = \mathbf{U}_2 \mathbf{\Sigma}_2 \mathbf{V}_2^T \tag{24}$$

After decomposition, the path channel vector $\mathbf{v}_1$ and $\mathbf{v}_2$ can be obtained from the first column of the matrix $\mathbf{V}_1$ and $\mathbf{V}_2$

$$\mathbf{v}_1 = \mathbf{V}_1(:, 1) \tag{25}$$

$$\mathbf{v}_2 = \mathbf{V}_2(:, 1) \tag{26}$$

Finally, we use channel vector replaces the nearest column vector in $\mathbf{F}_N$ and obtain $\mathbf{Q}_N$ after Schmidt orthogonalization. This process is shown in Fig. 4.

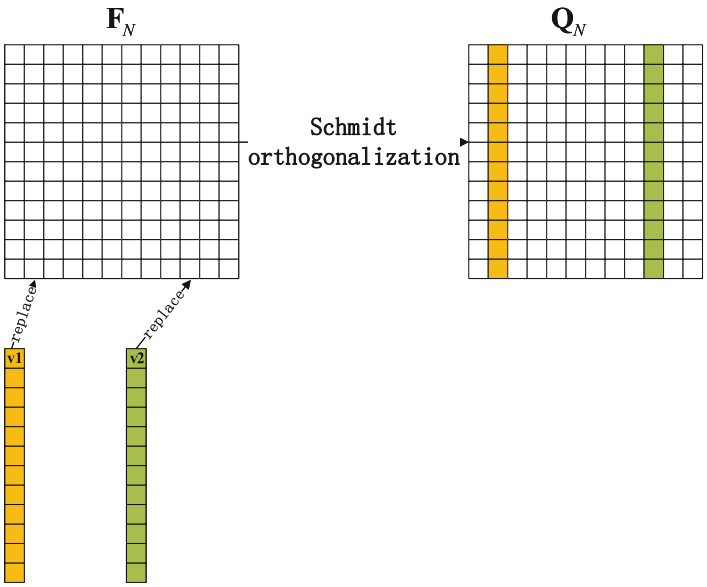

Fig. 4. Schematic diagram of adaptive orthogonal basis.

Compared with OTFS, the advantages of adaptive orthogonal basis scheme are improving the accuracy of channel estimation and reducing the cost of guard symbols by alleviating Doppler diffusion.

5 Simulation Results

In this section, we present the simulation results with coding and ideal channel estimation to compare the BER and BLER performance of our proposed scheme and OTFS. In addition, we show the performance of different symbols number N for the OTFS systems. Furthermore, the performance of different Doppler shifts feedback from the receiver is also shown.

The simulation setup is illustrated in Table 1. For channel model, we use two-path channel model, and the path delay, path Doppler and path power are $[0, 50/9]\,\mu$s, $[1.25, -3.125]$kHz and $[0, 0]$dB, respectively.

Table 1. Simulation Parameters

Parameter	Value
Carrier frequency	4 GHz
Number of subcarriers(M)	120
Number of symbols(N)	12
Subcarrier spacing(Δf)	15 kHz
CP length	$25/9\,\mu$s
Modulation	4-QAM

In Fig. 5, we compare the BER of different symbols number N in the Doppler domain. We use the channel estimation in [17] and compare the case of $N = 12$, $N = 24$ and $N = 48$. We can see that the performance is better as N increases. Obviously, the larger the N, the smaller the fractional Doppler effect [7]. In order to better verify the performance of our scheme, we limit the number of symbols to $N = 12$.

In Fig. 6, we compare the BER and BLER performance of the OTFS and our proposed adaptive orthogonal basis scheme. For fairness, we choose the ideal channel estimation with coding. It can be obtained that the adaptive orthogonal basis scheme has the advantage of alleviating Doppler diffusion without affecting performance. This advantage will further bring benefits, such as reducing pilot symbols expenses and obtaining channel estimation gains.

In practice, the Doppler shift feedback from the receiver is inaccurate, we further evaluate the performance of our scheme in the presence of Doppler error. We consider two Doppler error cases: ± 0.3 kHz and ± 1 kHz. In Fig. 7, we show the BER and BLER performance of our scheme with different Doppler error cases. We can see that the BER loss of two error cases at -2 dB are 0.1 dB and 0.2 dB respectively, the BLER loss are smaller. It can be obtained that our proposed scheme can work even when the number of symbols is limited and the Doppler shifts feedback from the receiver is inaccurate.

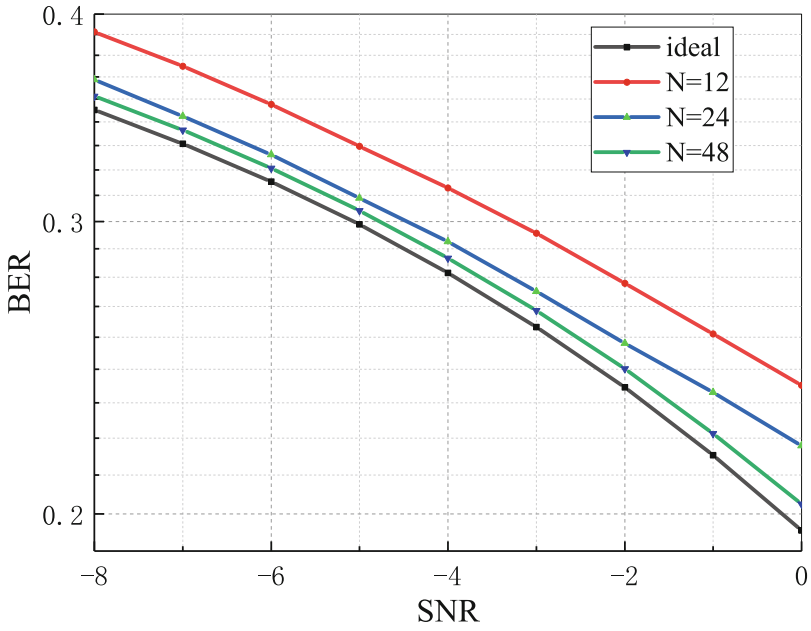

Fig. 5. The BER of different symbols number N in OTFS.

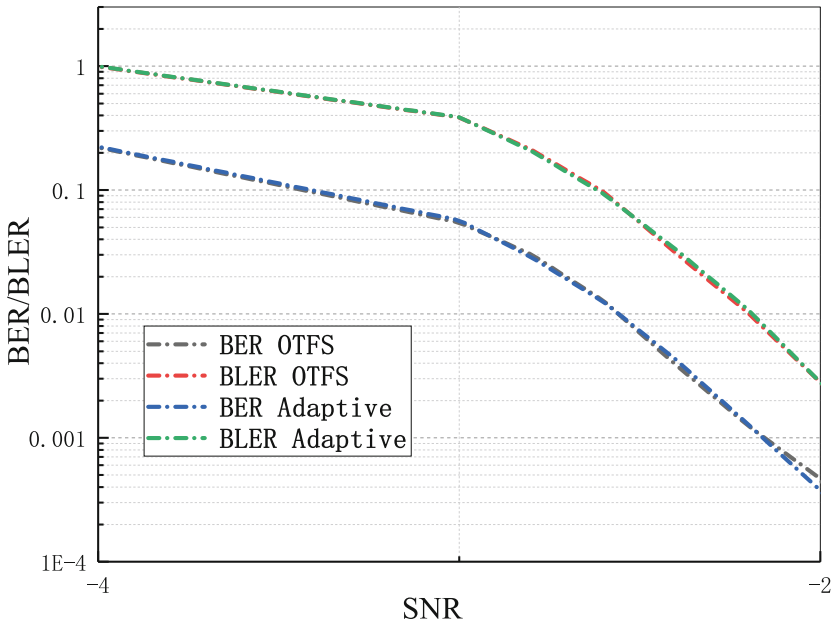

Fig. 6. The BER and BLER performance of the OTFS and our proposed scheme.

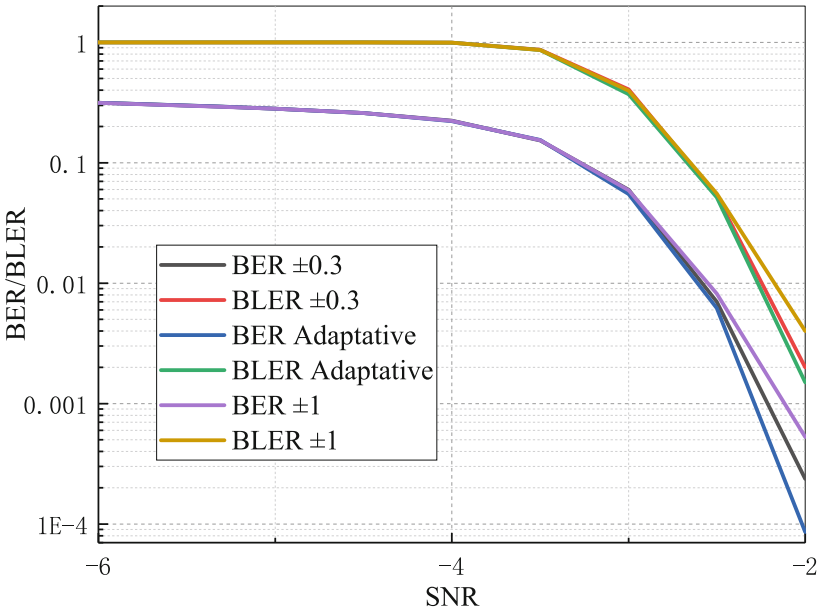

Fig. 7. The performance of our scheme with different Doppler error cases.

6 Conclusion

In this paper, we have analyzed the unavoidable fractional Doppler effects in the case of ideal waveform and show the cause of diffusion from both formula and geometric levels. In particular, we proposed an adaptive orthogonal basis scheme to alleviate the Doppler diffusion. In our scheme, we modified the matrix of the inverse symplectic finite Fourier transform by using the Doppler shifts feedback of the receiver. In the simulation results, we show that the BER and BLER performance of our proposed scheme are not affected compared with OTFS when coding and ideal channel estimation. And our scheme can work even when the number of symbols N is limited and the Doppler shifts feedback from the receiver is inaccurate.

ACKNOWLEDGEMENTS. This work is supported by National Natural Science Foundation of China (No. 61931005) and Beijing University of Posts and Telecommunications-China Mobile Research Institute Joint Innovation Center.

References

1. Hadani, R, et al.: Orthogonal Time Frequency Space Modulation. In: 2017 IEEE Wireless Communications and Networking Conference (WCNC), pp. 1–6(2016)
2. Hadani, R., et al.: Orthogonal Time Frequency Space (OTFS) modulation for millimeter-wave communications systems. In: 2017 IEEE MTT-S International Microwave Symposium (IMS), pp. 681–683(2017)

3. Zhiqiang, W., et al.: Orthogonal time-frequency space modulation: a promising next-generation waveform. IEEE Wirel. Commun. **28**(3), 136–144 (2021)
4. Khammammetti, V., Mohammed, S.: OTFS-based multiple-access in high doppler and delay spread wireless channels. IEEE Wireless Commun. Lett. **8**(2), 528–531 (2019)
5. Monk, A., Hadani, R., Tsatsanis, M., Rakib, S.: OTFS - Orthogonal Time Frequency Space. arXiv:1608.02993. (2016)
6. Saif Khan, M.: Derivation of OTFS modulation from first principles. IEEE Trans. Veh. Technol. **70**(8), 7619–7636 (2021)
7. Raviteja, P., Phan, K.T., Hong, Y., Viterbo, E.: Interference cancellation and iterative detection for orthogonal time frequency space modulation. IEEE Trans. Wireless Commun. **17**(10), 6501–6515 (2018)
8. Farhang, A., RezazadehReyhani, A., Doyle, L.E., Farhang-Boroujeny, B.: Low complexity modem structure for ofdm-based orthogonal time frequency space modulation. IEEE Wireless Commun. Lett. **7**(3), 344–347 (2018)
9. Murali, K. R., Chockalingam, A.: On OTFS modulation for high-doppler fading channels. In: 2018 Information Theory and Applications Workshop (ITA), pp. 1–10(2018)
10. Raviteja, P., Viterbo, E., Hong, Y.: OTFS performance on static multipath channels. IEEE Wireless Commun. Lett. **8**(3), 745–748 (2019)
11. Raviteja, P., Phan, K.T., Hong, Y.: Embedded pilot-aided channel estimation for OTFS in delay-doppler channels. IEEE Trans. Veh. Technol. **68**(5), 4906–4917 (2019)
12. Raviteja, P., Phan, K.T., Hong, Y., Viterbo, E.: Embedded delay-doppler channel estimation for orthogonal time frequency space modulation. In: 2018 IEEE 88th Vehicular Technology Conference (VTC-Fall), pp. 1–5 (2018)
13. Wenqian, S., Linglong, D., Jianping, A., Pingzhi, F., Robert, W.H.: Channel estimation for orthogonal time frequency space (OTFS) massive MIMO. IEEE Trans. Signal Process. **67**(16), 4204–4217 (2019)
14. 6G Vision and Candidate Technologies White Paper (2021). http://www.caict.ac.cn/english/news/202106/P020210608349616163475.pdf
15. Yiqing, Z., et al.: Service-aware 6G: an intelligent and open network based on the convergence of communication, computing and caching. Digital Commun. Netw. **6**(3), 253–260 (2020)
16. Yiqing, Z., Jiangzhou, W., Sawahashi, M.: Downlink transmission of broadband OFCDM Systems-part II: effect of Doppler shift. IEEE Trans. Commun. **54**(6), 1097–1108 (2006)
17. Yixiao, L. and Sen, W. and Jing, J. and Wei, X. and Hang, L.: Doppler Shift Estimation Based Channel Estimation for Orthogonal Time Frequency Space System. In: 2021 IEEE 94th Vehicular Technology Conference (VTC2021-Fall), pp. 1–6(2021)
18. Raviteja, P., Hong, Y., Viterbo, E., Biglieri, E.: Practical pulse-shaping waveforms for reduced-cyclic-prefix OTFS. IEEE Trans. Veh. Technol. **68**(1), 957–961 (2019)